Construction and characteristics of tandem organic solar cells featuring small molecule-based films on polymer-based subcells

2010 J. Phys. D: Appl. Phys. 43 025104

(http://iopscience.iop.org/0022-3727/43/2/025104)

IOP PUBLISHING JOURNAL OF PHYSICS D: APPLIED PHYSICS

J. Phys. D: Appl. Phys. **43** (2010) 025104 (8pp) doi:10.1088/0022-3727/43/2/025104

Construction and characteristics of tandem organic solar cells featuring small molecule-based films on polymer-based subcells

Fang-Chung Chen[1,3] **and Cheng-Hao Lin**[2]

[1] Department of Photonics and Display Institute, National Chiao Tung University, Hsinchu 30010, Taiwan
[2] Department of Photonics and Institute of Electro-Optical Engineering, National Chiao Tung University, Hsinchu 30010, Taiwan

E-mail: fcchen@mail.nctu.edu.tw

Received 4 August 2009, in final form 2 October 2009
Published 18 December 2009
Online at stacks.iop.org/JPhysD/43/025104

Abstract

In this study, we stacked a small molecule-based cell onto another polymer-based device to fabricate a tandem organic solar cell that extended the absorption range of the entire cell over a wider spectral range. Between the two subcells, we positioned a connecting structure comprising layers of Cs_2CO_3, Ag and MoO_3. Current matching phenomena played an important role in determining the device efficiency. The judicious selection of subcells exhibiting superior current matching improved the performance of the tandem cell. Indeed, in the optimally performing tandem cells we obtained both a high open-circuit voltage (1.21 V) and an improved power conversion efficiency (1.81%). From analyses of the surface morphology and transmission spectra of the middle Ag layers, we deduced that the main function of this film was to provide more sites for efficient recombination of holes and electrons. The thickness of this layer was limited by its transmittance. A thinner Ag layer allowed more light to be harvested by the top cell, increasing the overall performance of the tandem cell.

(Some figures in this article are in colour only in the electronic version)

1. Introduction

Organic photovoltaic devices offer the advantageous features of light weight, low cost and mechanical flexibility to their applications in solar energy conversion [1–5]. The most efficient organic solar cells reported so far have been fabricated based on donor–acceptor heterojunction structures [6, 7]. Because of the high binding energy, excitons generated upon light absorption in organic semiconductors can only be dissociated into free electrons and holes at such heterojunctions between two materials possessing opposite electron affinities; this dissociation event contributes to the photocurrent. The power conversion efficiency (PCE) of organic solar cells containing heterojunctions has been improved recently up to ca 6% [8, 9]. Further improvements will require solving some fundamental problems associated with organic materials—such as the low mobility and limited absorption range of single organic materials—in order to meet the high efficiency required for practical applications.

To extend the spectral coverage of the photoactive layers, tandem solar cells, or devices featuring multiple junctions, have been studied widely since 1990 [10]. Different materials possessing various absorption ranges are employed together in the semiconducting layers of the individual cells; these subcells are connected in series by intermediate layer(s). Enhanced spectral coverage can be achieved through superposition of the absorption spectra of these layers in different subcells. For example, Hiramoto *et al* presented an early study of small-molecule-based tandem

[3] Author to whom any correspondence should be addressed.

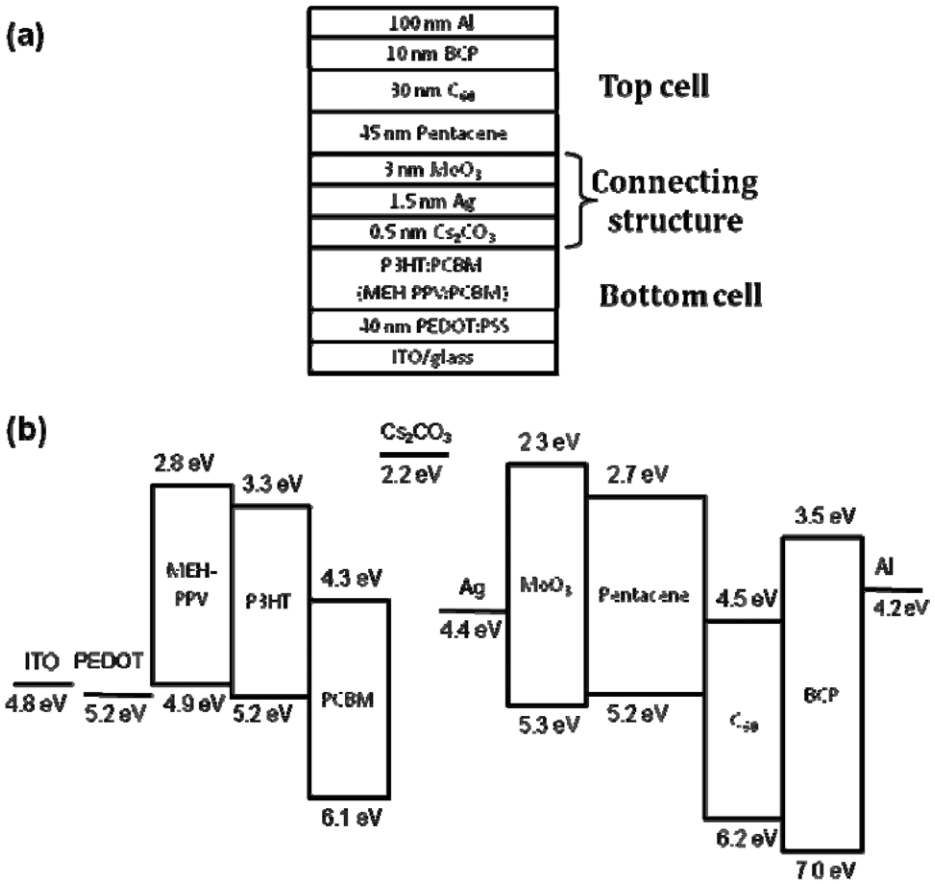

Figure 1. (*a*) Device structure of the organic tandem solar cell. (*b*) Energy level diagram of the materials used in this study.

devices connected through a semitransparent Au interlayer [10]. Yakimov and Forrest stacked two cells with ultrathin layers of Ag nanoclusters, which served as recombination centres for unpaired charges from the subcells [11]. Hybrid structures, consisting of thermally evaporated small-molecule and solution-processed polymer layers, have also been developed [12, 13]. More recently, a solution-processed tandem cell exhibiting complementary absorptions in each subcell was demonstrated by connecting subcells through a composite interlayer to prevent dissolution of the bottom layers [14, 15]. Kim *et al* fabricated tandem solar cells through all-solution processing and achieved a remarked PCE of 6.5% [8]. Nevertheless, systematic investigations of the device characteristics and relevant physics remain rare, especially for devices containing hybrid structures. In this study, we used poly(3-hexylthiophene) (P3HT) and poly[2-methoxy-5-(2′-ethylhexyloxy)-1,4-phenylenevinylene] (MEH-PPV) as electron donor materials and [6, 6]-phenyl-C_{61}-butyric acid methyl ester (PCBM) as an electron acceptor for the fabrication of bottom cells; for the top cells, we used the small-molecule pentacene as the electron donor and fullerene (C_{60}) was used as the electron acceptor (figure 1). We employed evaporation of pentacene to avoid possible interlayer mixing during a spin-coating process used to fabricate the top cells. For the intermediate (connecting) layers, we used a trilayer structure to link the cells. With this model device structure in hand, we systematically investigated the optical and electrical properties of the organic tandem cells.

2. Experimental details

Figure 1(*a*) depicts the device structure of the tandem cells; figure 1(*b*) presents the energy levels of the materials used in this study and work functions of the electrodes. The devices were prepared on patterned indium tin oxide (ITO)-coated glass substrates. The ITO substrates were cleaned sequentially with a detergent, acetone and isopropanol. After cleaning, the substrates were dried in an oven. Prior to deposition of the organic layers, the substrates were further treated with UV-ozone for 15 min. For the fabrication of the bottom cell, poly(3,4-ethylenedioxythiophene) : poly(styrenesulfonate) (PEDOT : PSS) was spin-coated onto the substrates. After thermal annealing of the PEDOT : PSS layer at 120 °C for 1 h, the active polymer layer, consisting of either P3HT and PCBM (1 : 1, w/w) or MEH-PPV and PCBM (1 : 4, w/w) dissolved in 1,2-dichlorobenzene, was deposited on top of the PEDOT : PSS layer. For the P3HT : PCBM and MEH-PPV : PCBM films, the substrates were thermally annealed at 110 °C for 15 min and at 70 °C for 30 min, respectively. After deposition of the polymer layers, the connecting structure was deposited through sequential thermal evaporation of layers of Cs_2CO_3 (0.5 nm), Ag (1.5 nm) and MoO_3 (3.0 nm). A 45 nm thick electron donor layer of pentacene was then deposited, followed by a 30 nm thick electron acceptor layer of C_{60}. Next, a 10 nm thick layer of bathocuproine (BCP) was deposited as an exciton blocking layer. Finally, Al (100 nm) was deposited through

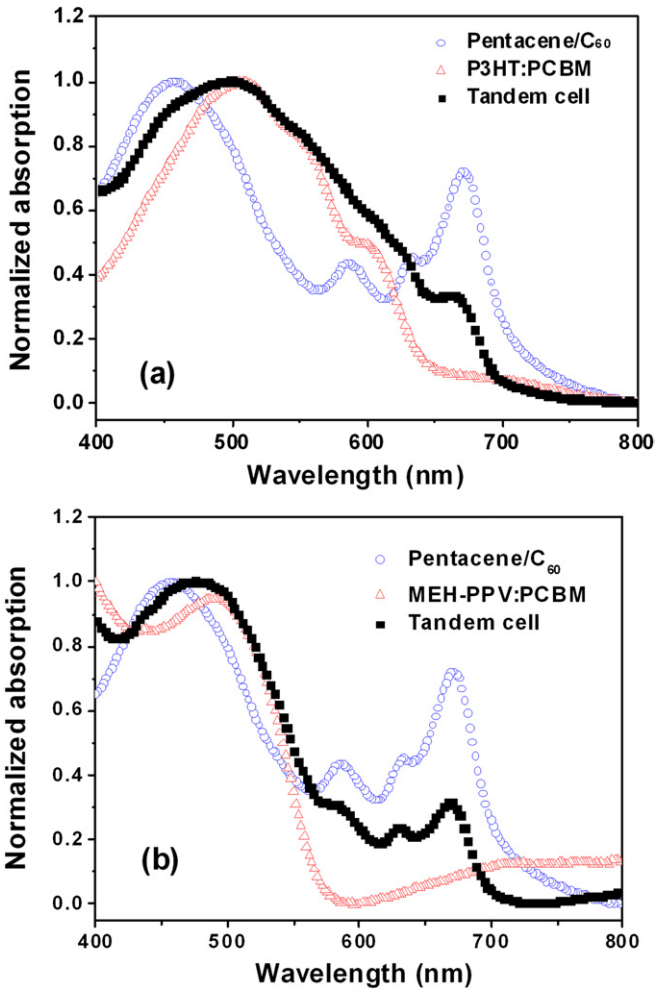

Figure 2. (*a*) Absorption spectra of the photoactive layers in the single P3HT : PCBM reference cell, the pentacene/C_{60} reference cell and the tandem cells. (*b*) Absorption spectra of the photoactive layers in the single MEH-PPV : PCBM reference cell, the pentacene/C_{60} reference cell and the tandem cells.

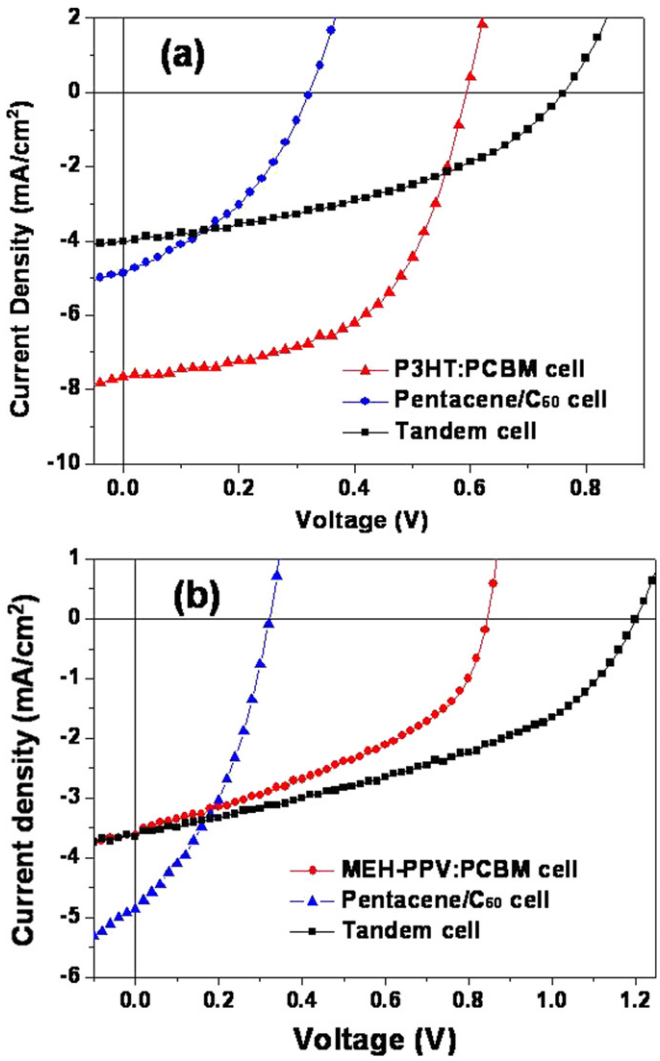

Figure 3. *J*–*V* characteristics of the single reference cells and the tandem cell under 100 mW cm^{-2} illumination (AM 1.5G). Conjugated polymers used in these devices: (*a*) P3HT; (*b*) MEH-PPV.

a shadow mask to define the device area. The device current density–voltage (*J*–*V*) curves were obtained using a Keithley 2400 source-measure unit. The measurements of the device characteristics were performed under illumination (100 mW cm^{-2}, AM 1.5G) with light provided by a solar simulator (Oriel 150W). The illumination intensity was calibrated using a standard Si photodiode detector equipped with a KG-5 filter [16]. The absorption spectra were obtained using a Perkin–Elmer Lambda 650 spectrometer. The thin film morphology was visualized using a DI 3100 series atomic force microscope (AFM).

3. Results and discussion

3.1. Optical and electrical properties of the tandem cells

Figure 2(*a*) presents the absorption spectra of the various organic layers as well as the overall absorption of the as-made tandem cells. The major absorption of the P3HT : PCBM layer was located between 400 and 600 nm. The pentacene/C_{60} bilayer structure featured two major absorption peaks: one at ca 400–500 nm and the other at 600–700 nm. By combining the polymer and small-molecule layers, the absorption spectrum of the tandem cell was extended to cover almost the entire visible spectrum. Figure 2(*b*) displays the absorption spectra of the other photoactive polymer layers (MEH-PPV and PCBM blend). The main absorption peak of MEH-PPV was located at ca 480 nm, slightly blue shifted relative to that of P3HT. Similarly, the absorption of the tandem cell prepared from MEH-PPV : PCBM blends could also be extended to ca 700 nm.

Figure 3(*a*) displays the *J*–*V* characteristics under illumination (100 mW cm^{-2}, AM 1.5G) of the tandem cell in which the polymer bottom cell comprised the polymer blend consisting of P3HT and PCBM. The cell exhibited an open-circuit voltage (V_{oc}) of 0.77 V, a short circuit current (J_{sc}) of 4.01 mA cm^{-2} and a fill factor (FF) of 40%. The PCE was calculated to be 1.24%. Figure 3(*a*) also shows the *J*–*V* curves of the corresponding reference single cells. For the small molecule-based reference cell, the values of V_{oc}, J_{sc}

Table 1. Electrical properties of the devices in this study.

Cell type	V_{oc} (V)	J_{sc} (mA cm^{-2})	FF (%)	PCE (%)
P3HT : PCBM reference cell: ITO/PEDOT/P3HT:PCBM(80 nm)/Cs_2CO_3(0.5 nm)/Al(100 nm)	0.59	7.67	56	2.51
MEH-PPV : PCBM reference cell: ITO/PEDOT/MEH-PPV:PCBM(100 nm)/Cs_2CO_3(0.5 nm)/Al(100 nm)	0.85	3.62	41	1.27
Small molecule-based reference cell: ITO/MoO_3/pentacene (45 nm)/C_{60} (30 nm)/BCP (10 nm)/Al(100 nm)	0.33	4.86	38	0.61
Tandem cell: ITO/PEDOT/P3HT:PCBM (80 nm)/Cs_2CO_3 (0.5 nm) /Ag (1.5 nm)/MoO_3 (3 nm)/pentacene (45 nm)/C_{60} (30 nm)/BCP (10 nm)/Al (100 nm)	0.77	4.01	40	1.24
Tandem cell: ITO/PEDOT/MEH-PPV : PCBM (100 nm)/Cs_2CO_3(0.5 nm)/Ag (1.5 nm)/ MoO_3 (3 nm)/pentacene (45 nm)/C_{60} (30 nm)/BCP (10 nm)/Al (100 nm)	1.21	3.65	41	1.81

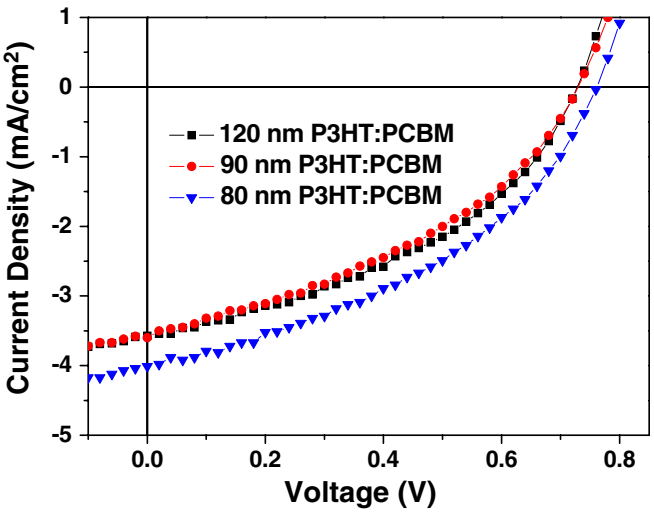

Figure 4. J–V characteristics of the tandem cells prepared with different thicknesses of P3HT : PCBM polymer layers under illumination (AM 1.5G, 100 mW cm^{-2}).

and FF were 0.33 V, 4.86 mA cm^{-2}, and 38%, respectively, yielding a PCE of 0.61%. The corresponding polymer single cell exhibited superior performance, with values of V_{oc}, J_{sc} and FF of 0.59 V, 7.67 mA cm^{-2}, and 56%, respectively; its calculated PCE was 2.51%. Note that the efficiency of the small-molecule cell was slightly lower [17–19]. A higher efficiency is expected after we purify the organic compounds. Although the tandem cell had a higher value of V_{oc}, its PCE was worse than that of the single P3HT : PCBM cell because of the lower values of its photocurrent and FF. We also note that the value of V_{oc} of the tandem device was less than the sum of open-circuit voltages of the individual reference cells. Table 1 summarizes the device structures and their electrical properties.

3.2. Current matching

One of the critical issues for achieving high efficiency in tandem cells is current matching between the two subcells [15]. Figure 4 displays the J–V characteristics of the tandem cells prepared using different thicknesses of the P3HT : PCBM layers. The short-circuit current decreased with increasing thickness. One should note that the best condition for the P3HT : PCBM-based device was around ∼200 nm [20]. In contrast, for the tandem cells, the optimal thickness of the P3HT : PCBM layer was 80 nm in this study. The polymer-based bottom subcell probably required a lower photocurrent to match that of the top subcell to obtain the higher PCE of the tandem cell [15]. Because the photocurrent of the polymer-based cell was higher than that of the small molecule-based subcell, the excess electrons from the former could not recombine with the holes from the latter, thereby resulting in charging of the middle electrode. Therefore, the charges compensated the built-in voltage in the device and resulted in a reduced value of V_{oc} of the tandem cell.

For achieving better current matching, rather than using a P3HT : PCBM subcell, we employed an MEH-PPV : PCBM device, which exhibited a higher value of V_{oc} (0.85 V) and a lower value of J_{sc} (3.62 mA cm^{-2}) [21], to match the top small molecule-based subcell. Figure 3(*b*) displays the J–V characteristics of the tandem cell and the reference cells. As expected, the resulting value of V_{oc} of the tandem cell was 1.21 V, close to the sum of the voltages of the reference cells. Because the photocurrent of the subcells was more closely matched, we obtained higher efficiency (1.81%). Table 1 also summarizes the electrical properties of this system.

3.3. Effect of the illumination intensity

Figure 5 displays the dependences of the values of V_{oc}, J_{sc} and PCE of the reference cells and the tandem cell on the intensity of the incident light. The maximum value of V_{oc} of each cell was obtained at a different light intensity. For all the devices, the open-circuit voltages gradually increased with the light intensity up to ca 1 sun, becoming almost saturated thereafter (figure 5(*a*)). In addition, the short-circuit current also increased with increasing light intensity (figure 5(*b*)). Interestingly, the values of J_{sc} of the tandem cell were either equal to or smaller than those of the reference polymer- and small molecule-based cells, following the lower value up to ca 2.5 sun. We attribute this phenomenon to current matching, as described above. When the light intensity was greater than 2.5 sun, however, the current was further limited; in this case, the values of J_{sc} of the tandem cell were lower than those of both the polymer- and small molecule-based cells. Although

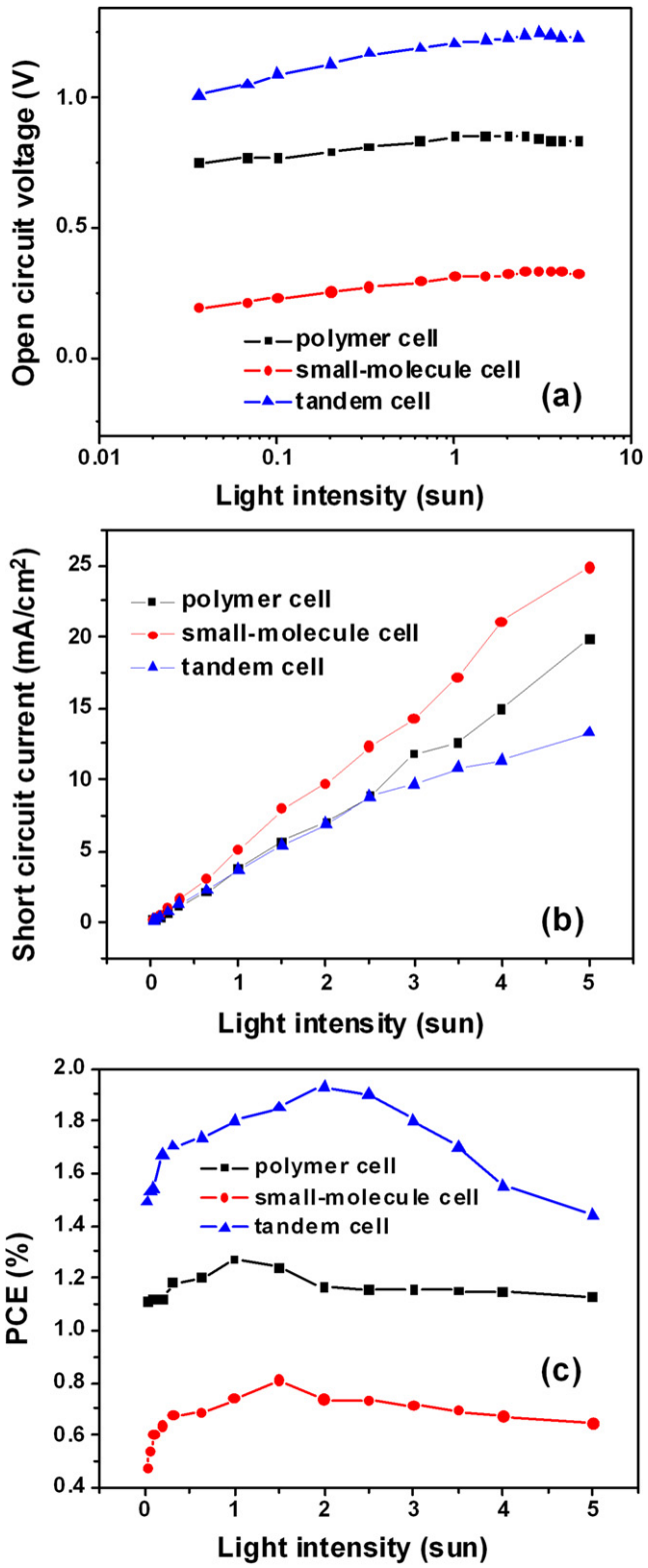

Figure 5. Dependence of the values of (*a*) V_{oc}, (*b*) J_{sc} and (*c*) PCE of the reference cells and the tandem cell on the intensity of the incident light. The conjugated polymer used in these devices was MEH-PPV.

we are still investigating these interesting phenomena, we suspect that the photocurrent might be further limited by the recombination efficiency of the middle Ag layer at high illumination intensity.

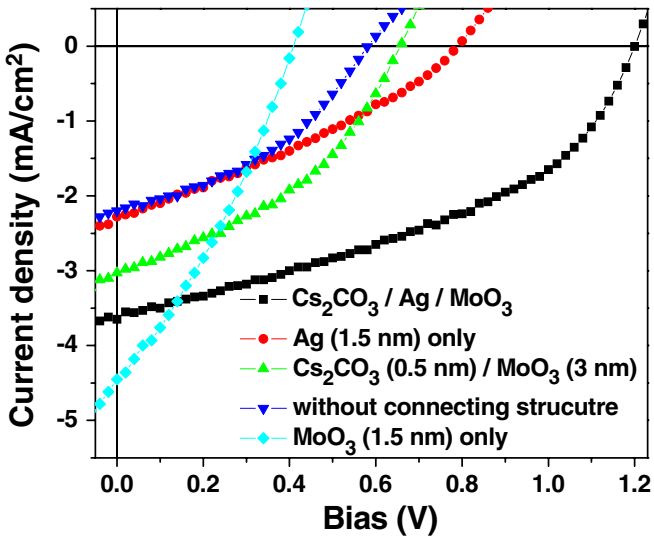

Figure 6. *J*–*V* characteristics of tandem cells prepared with various interlayer structures under 100 mW cm^{-2} illumination (AM 1.5G). The conjugated polymer used in these devices was MEH-PPV.

Figure 5(*c*) indicates that while the maximum efficiencies of the reference polymer- and small molecule-based cells were obtained under illumination at 1 sun and 1.5 sun, respectively, the maximum efficiency of the tandem cell (1.93%) occurred under 2 sun. We suspect that when the incident light intensity was stronger, more light passed through the polymer subcell to be absorbed by the small molecule-based top subcell. Because the top cell limited the overall device current, more current could be extracted from the tandem cell when stronger illumination was applied; in turn, this phenomenon enhanced the PCE of the tandem cell. Therefore, we infer that some optical structures on photovoltaic devices could be further designed to concentrate the incident light to increase the performance of the tandem cells.

3.4. Effect of the middle electrode

To further investigate the functions of the connecting structure, we prepared tandem cells incorporating different connecting layers. Figure 6 reveals that the tandem device fabricated without any connecting layer exhibited very low values of V_{oc} and J_{sc}. Even we added functional layers of MoO_3 and Cs_2CO_3 in an attempt to form ohmic contacts with both subcells, the subcells remained poorly connected: the open-circuit voltage of the tandem cell was only 0.65 V. The subcells were only effectively connected after we constructed a trilayer electrode structure, suggesting that a charge recombination zone (Ag layer) was essential feature of an efficient tandem cell. On the other hand, when we incorporated only a thin Ag layer between the subcells, the value of J_{sc} remained severely limited, although the value of V_{oc} was larger than those of the other devices (figure 6). These results indicate that electrode modification layers, i.e. MoO_3 or Cs_2CO_3, were also the other essential features leading to lower resistance between the contacts. In short, because the interlayers (MoO_3 and Cs_2CO_3) and the middle Ag layer were all required, we conclude that an effective connecting structure should perform two functions

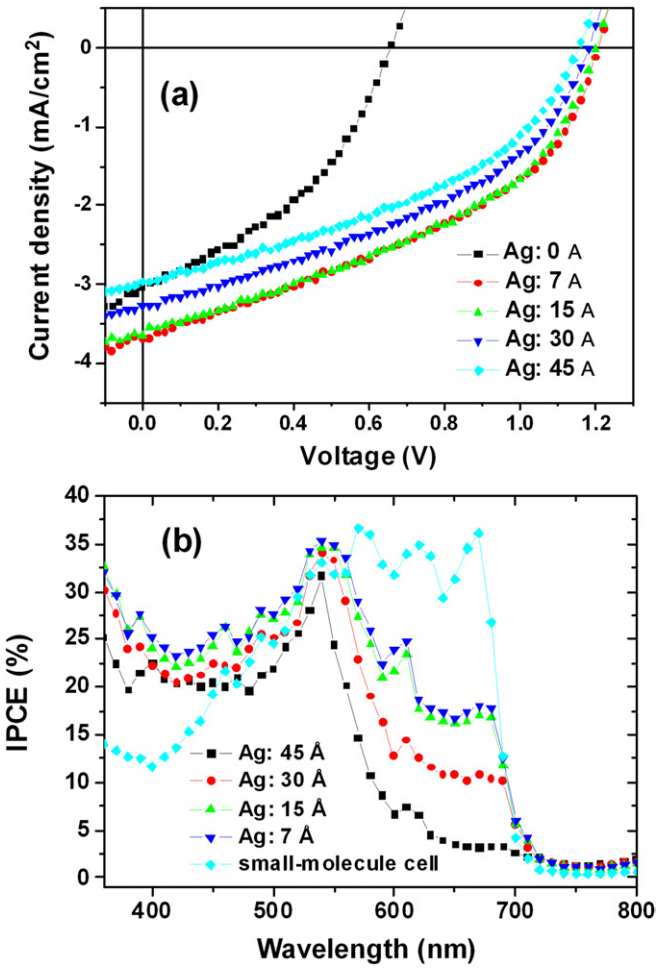

Figure 7. (*a*) *J*–*V* characteristics of tandem cells prepared with various thicknesses of the middle Ag layers under 100 mW cm^{-2} illumination (AM 1.5G). Device structure: ITO/PEDOT/MEH-PPV : PCBM (100 nm)/Cs_2CO_3 (0.5 nm)/Ag (x nm)/MoO_3(3 nm)/pentacene (45 nm)/C_{60} (30 nm)/BCP (10 nm)/Al (100 nm). (*b*) IPCE spectra of the tandem cells prepared with various thicknesses of the Ag interlayers, compared with that of the small molecule-based reference cell.

simultaneously: it should serve as a recombination centre and reduce the injection barriers for electrons and holes at the interfaces between the interlayers and the organic thin films.

To understand the function of the middle Ag layer, we prepared tandem cells incorporating different thicknesses of this layer. Figure 7(*a*) displays the resulting device performances. While the thickness of the Ag layer decreased from 45 to 7 Å, the value of J_{sc} increased from 2.79 to 3.68 mA cm^{-2}, the value of V_{oc} increased from 1.15 to 1.21 V and the FF decreased slightly to 40%. The highest PCE was obtained while the Ag thickness was 15 Å. Table 2 provides a summary of the electrical properties.

From the slopes of the *J*–*V* curves recorded in the dark, we calculated the device series resistances (R_s) of the devices featuring different Ag layer thicknesses (table 2) [22, 23]. Unexpectedly, we found that the value of the device R_s increased gradually from 5.51 to 8.51 Ω cm^2 with an increase in the thickness of the Ag layer from 7 to 45 Å. The major contributors to the value of R_s were the contact resistances

Table 2. Electrical properties of the tandem cells with various middle Ag layer thicknesses.

Ag thickness (Å)	V_{oc} (V)	J_{sc} (mA cm^{-2})	FF (%)	PCE (%)	R_s (Ω cm^2)
45	1.15	2.79	41	1.4	8.51
30	1.17	3.26	41	1.57	7.01
15	1.21	3.65	41	1.81	6.57
7	1.21	3.68	40	1.8	5.51

between the layers and the bulk resistance of each layer. The value of the contact resistance is influenced by the interface between the electrodes and the organics. Because the bulk resistance remained unchanged after increasing the thickness of the Ag layer, the increase in R_s presumably resulted from property changes at the middle electrode.

To understand the reason for the increased value of R_s, we recorded AFM images of the Ag layers on the bottom cells. When a 7 Å thick layer of Ag was deposited on the surface, the AFM images indicated that the Ag formed isolated clusters (figure 8(*a*)). Even the 45 Å thick Ag 'layer' was not continuous (figure 8(*d*)). Such nanocluster layers would trap charges readily; subsequently, the attracted opposite charges would enhance the recombination process [24]. On the other hand, the buildup of the space charges possibly increased the device series resistance, especially in the absence of illuminating light. In other words, the major function of the middle Ag layer was not to directly 'connect' the subcells; rather, the Ag nanoclusters provided more efficient sites for recombination of holes and electrons from the top and bottom subcells, respectively.

Figure 8 reveals that Ag nanoclusters formed when the Ag thickness was less than 45 Å. To understand why the optimized Ag layer thickness was less than ca 15 Å, we measured the transmittance spectra of these solar cells incorporating different Ag layer thicknesses (figure 9). The average transmittance of the Ag layer in the wavelength range 400–800 nm increased from 57% to 91% when the thickness of the Ag layer decreased from 45 to 7 Å. With the incident light being introduced from the bottom ITO electrode, more photons could transmit through the Ag layer and could be absorbed by the bottom pentacene/C_{60} subcell when the Ag layer was thinner. Because the PCE of the small molecule-based top cell increased up to an illumination of ca 1.5 sun (figure 5(*c*)), we deduced that the overall performance of the tandem cell improved when the top cell could harvest more photons under the standard illumination conditions (1 sun).

To further confirm our hypothesis, we measured the incident photon-to-electron conversion efficiency (IPCE) of the devices prepared with different thicknesses of the middle Ag layer (figure 7(*b*)). The small molecule-based reference cell is also included for easier comparison. Note that the major absorption of the MEH-PPV : PCBM active layer was located below 550 nm and the layers of pentacene/C_{60} exhibited a significant absorption between 500 and 700 nm (figure 2(*b*)). In figure 7(*b*) we clearly observe that the contribution of the photocurrent from the small molecule-based subcell decreased with increasing thickness of the middle Ag layer, suggesting

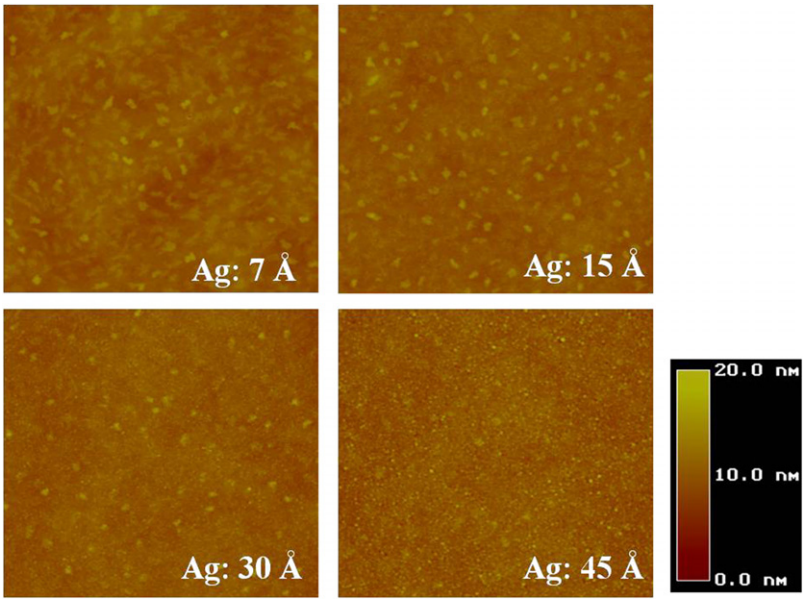

Figure 8. AFM images ($3 \times 3\ \mu m^2$) of the Ag layers on the bottom cells, which had the structure ITO/PEDOT/MEH-PPV : PCBM (100 nm)/Cs_2CO_3 (0.5 nm).

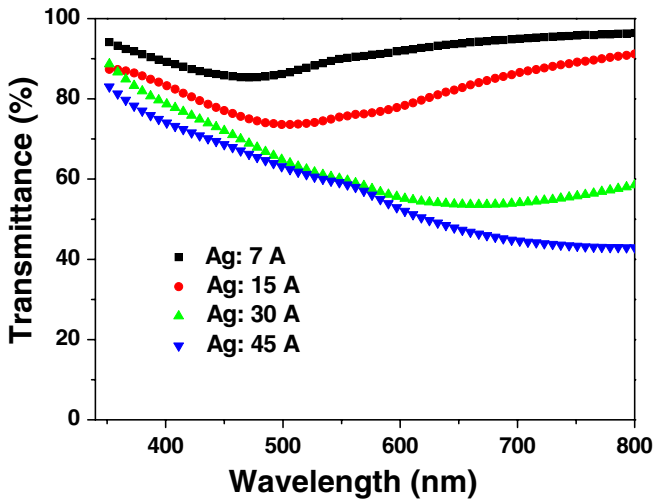

Figure 9. Transmittance spectra of Ag interlayers of various thicknesses.

that fewer photons could pass through this layer. Therefore, when the thickness of the Ag was 45 Å, for example, the smaller photocurrent generated from the top cell limited the overall current of the tandem cell because of the current matching phenomenon, thereby decreasing the PCE.

4. Conclusion

We have prepared organic tandem solar cells by stacking polymer- and small molecule-based subcells together through an effective connecting structure comprising Cs_2CO_3, Ag and MoO_3 layers. Whereas the photoactive layer of the polymer subcell mainly absorbed photons having wavelengths of less than 600 nm, the small molecule-based layer of the top cell exhibited significant absorptions well beyond 600 nm, thereby extending the overall absorption regime. We found that a current matching phenomenon played an important role in determining the device efficiency. Although the P3HT : PCBM single-layer device had a higher photocurrent and PCE, the performance of the tandem cell prepared from the P3HT : PCBM subcell was worse than that of one made from the MEH-PPV : PCBM subcell. Although the single-layer (reference) cell incorporating MEH-PPV as the photoactive polymer exhibited a lower photocurrent, it was a much better match for that of the small molecule-based top cell. As a result, this system achieved both a high open-circuit voltage (1.21 V) and a high PCE (1.81%). From analyses of the device characteristics and transmission spectra of the Ag layers, we deduced that the main function of the middle metal layer was to provide more sites for efficient recombination of holes and electrons. The thickness of such a layer is, however, limited by its transmittance. When the Ag layer was thin, more light was harvested by the top cell, thereby increasing the overall performance of the tandem cell.

Acknowledgments

The authors thank the National Science Council (NSC 98-2221-E-009-028 and NSC-96-ET-7-009-001-ET) and the Ministry of Education (through the ATU program) for financial support.

References

[1] Dennler G, Scharber M C and Brabec C J 2009 *Adv. Mater.* **21** 1323
[2] Chen L M, Hong Z, Li G and Yang Y 2009 *Adv. Mater.* **21** 1434
[3] Peet J, Senatore M L, Heeger A J and Bazan G C 2009 *Adv. Mater.* **21** 1521
[4] Ko C J, Lin Y K and Chen F C 2007 *Adv. Mater.* **19** 3520
[5] Chan M Y, Lai S L, Fung M K, Lee C S and Lee S T 2007 *Appl. Phys. Lett.* **90** 023504
[6] Tang C W 1986 *Appl. Phys. Lett.* **48** 183

[7] Yu G, Gao J, Hummelen J C, Wudl F and Heeger A J 1995 *Science* **270** 1789
[8] Kim J Y, Lee K, Coates N E, Moses D, Nguyen T-Q, Dante M and Heeger A J 2007 *Science* **317** 222
[9] Park S H, Roy A, Beaupré S, Cho S, Coates N, Moon J S, Moses D, Leclerc M, Lee K and Heeger A J 2009 *Nature Photon.* **3** 297
[10] Hiramoto M, Suezaki M and Yokoyama M 1990 *Chem. Lett.* 327
[11] Yakimov A and Forrest S R 2002 *Appl. Phys. Lett.* **80** 1667
[12] Dennler G, Prall H, Koeppe R, Egginger M, Autengruber R and Sariciftci N S 2006 *Appl. Phys. Lett.* **89** 073502
[13] Colsmann A, Junge J, Kayser C and Lemmer U 2006 *Appl. Phys. Lett.* **89** 203506
[14] Hadipour A, de. Boer B and Blom P W M 2007 *J. Appl. Phys.* **102** 074506
[15] Hadipour A, de Boer B, Wildeman J, Kooistra F B, Hummelen J C, Turbiez M G R, Wienk M M, Janssen R A J and Blom P W M 2006 *Adv. Funct. Mater.* **16** 1897
[16] Shrotriya V, Li G, Yao Y, Moriarty T, Emery K and Yang Y 2006 *Adv. Funct. Mater.* **16** 2016
[17] Yoo S, Domercq B and Kippelen B 2005 *J. Appl. Phys.* **97** 103706
[18] Cheyns D, Gommans H, Odijk M, Poortmans J and Heremans P 2007 *Sol. Energy Mater. Sol. Cells* **91** 399
[19] Yang J and Nguyen T Q 2007 *Org. Electron.* **8** 566
[20] Li G, Shrotriya V, Huang J, Yao Y, Moriarty T, Emery K and Yang Y 2005 *Nature Mater.* **4** 864
[21] Chen F C, Xu Q and Yang Y 2004 *Appl. Phys. Lett.* **84** 3181
[22] Johnston W D 1980 *Sol. Voltaic Cells* (Dekker: New York)
[23] Sievers D W, Shrotriya V and Yang Y 2006 *J. Appl. Phys.* **100** 114509
[24] Rand B P, Peumans P and Forrest S R 2004 *J. Appl. Phys.* **96** 7519